

## Developing a Predictive Weld-Seam Formation Model: Experimental Support

A.J. den Bakker<sup>1</sup>, R.J. Werkhoven<sup>2</sup>, W.H. Sillekens<sup>2</sup>, L. Katgerman<sup>3</sup>

<sup>1</sup> Nedal Aluminium, Utrecht, The Netherlands

<sup>2</sup> TNO Science & Industry, Eindhoven, The Netherlands

<sup>3</sup> Delft University of Technology, Delft, The Netherlands

### Abstract

In hollow aluminium extrusions produced with porthole dies, longitudinal weld-seams are present throughout the entire extruded length, due to rejoining of metal streams inside the extrusion tooling. These weld-seams, formed by a solid-state bonding process at elevated temperatures and under conditions of interfacial pressure and plastic deformation, are commonly the weakest areas in the extrusion cross-section. Therefore, predictive control of the weld-seam formation process is essential. For this purpose a conceptual model is developed, containing all relevant features pertaining to the solid-state bonding process as this occurs in aluminium extrusion.

This paper describes an experimental programme aimed at exploring the effects of tooling geometry, process conditions and alloy composition on weld-seam performance. In lab-scale experiments, strips were extruded from AA6060 and AA6082 billets, using tooling geometries in which a bridge was incorporated to form a weld-seam. Keeping the profile geometry constant, the internal geometry of the tooling was varied, resulting in different bonding conditions. The obtained weld-seams were characterised by means of transverse tensile tests. Associated microstructural characterisation of the extrusions and inspection of fracture surfaces was performed in order to relate the mechanical performance to microstructural features.

The results clearly show that the evolutionary microstructural response of the alloy, determined by the local thermomechanical conditions inside the die, has a significant effect on the weld-seam performance. It is therefore concluded that, besides a criterion for suitable flow conditions and interfacial pressure, a predictive tool for weld-seam quality must incorporate the evolutionary microstructural response of the alloy in question.

**Keywords:** *Extrusion, Weld-seam, Solid-state bonding, Ductility index*

### Introduction

In aluminium extrusion a pre-heated billet is pressed through a die orifice with the desired geometry, resulting in an elongated section with a constant cross-sectional geometry. Hollow sections are generally produced with dies in which a core, or mandrel, is internally suspended in the die by means of legs or bridges. Given the geometrical flexibility and the efficiency of use, porthole dies are the most common tooling configuration for the production of (multi-)hollow sections. In extrusion through porthole dies, longitudinal weld-seams are formed when the aluminium, after being split into separate metal streams flowing around the legs, rejoin in the welding chambers. The joining of the metals streams occurs under conditions of pressure, strain/shear and temperature, but without the occurrence of liquid phases; i.e. a solid-state bonding process. Influenced by the particular local process conditions, micro-structural reorganisation processes such as recovery, recrystallisation and grain growth occur, having an obvious bearing on the properties of a weld-seam for a given alloy.

If the combination of the local processing parameters is unfavourable, weld-seam defects occur. These range from porosity (when air or gas is entrapped, or when voids are formed in the aluminium bulk, as described by Akeret [1] and Valberg et al. [2]) and contamination by foreign matter on the weld-seam bond plane to cases where inferior mechanical performance of the weld-seams occurs. In these last cases, the particular underlying defect may not be obvious from visual observation, as is particularly the case for so-called 'kissing bonds' described by Oosterkamp et al. [3].

It should be noted that the actual properties of weld-seams may differ from those of the parent material. Not necessarily does this infer that an inferior bond is formed, as the discussion arises according to which method the weld seam properties should be assessed and which criteria should be applied in evaluating the weld-seam properties. Nevertheless, in general the goal is to produce weld-seams with properties similar to those of the other parts of the section. For this purpose it is necessary to predictably control the performance of weld-seams in extrusion.

### Prediction of bond performance

The formation of weld-seams has been addressed by several others, often utilising numerical techniques to calculate the local conditions in the welding chamber, resulting in a conclusion concerning the weld-seam quality. Under the presumption of suitable flow conditions, several methods have been developed to relate the particular operating conditions and tooling geometry to the resulting weld-seam integrity. Many of these methods centre on a mechanical interpretation of the solid-state bonding process; that is, for achieving an adequate level of pressure on the welding plane, as described in a comprehensive review by Donati et al. [4]. For specific well-defined conditions, the outcome of these models – expressed by a value for the weld-seam criterion – can be correlated with experimental results. These criteria give a global indication of weld-seam quality, thereby disregarding particular cases where only partial bond formation occurs on the weld plane. Consequently, a truly comprehensive treatment of the weld-seam formation process must take into account all prerequisites for bonding, notably: 1) fully converging metal flow in the die to ensure sustained contact between the rejoining streams along the entire bonding path, 2) a pressure on the bonding plane that exceeds a particular threshold value to ensure sustained contact, and 3) micro-structural reorganisation to ensure atomic registry of the bonding plane. These factors are to be incorporated in a weld-seam integrity function  $I_{ws}$  as described below.

In the case of weld seam formation, we consider the bonding plane (i.e., the evolving contact surface between the rejoining metal streams) as a distribution of  $N$  elements, with a discrete “snap” function  $W_i$ . Depending on the local conditions, the processing history and micro-structural evolution, each element is assigned a discrete value, designating a non-bonding ( $W_i=0$ ) or bonding ( $W_i=1$ ) status. The weld-seam integrity  $I_{ws}$  is then defined by:

$$I_{ws} = \frac{1}{N} \sum_{i=0}^{i=N} W_i \quad (1)$$

The weld-seam property  $P_{ws}$  is related to the bond property  $P_b$  of the bulk material:

$$P_{ws} = \alpha I_{ws} P_b \quad (2)$$

Thus, for a fully bonded structure  $I_{ws} = 1$ . For  $I_{ws} = 0$ , and hence  $P_{ws} = 0$ , no bond is formed. For other values of  $I_{ws}$  the weld seam will possess intermediate property values. These are not necessarily proportional to  $I_{ws}$ , as indicated by  $\alpha$ , a factor related to the damage mechanism causing the weld seam to fail.

Assessment of the bond relies on measuring a quantified value for the bond performance. Many previous studies have utilised static strength values (i.e., yield stress and/or ultimate tensile stress) determined from uniaxial tensile tests for this purpose; however, these values do not always reflect the true performance of a weld seam.

### Experimental

The extrusion experiments were conducted using a 500 kN laboratory extrusion press operating in the direct mode. Billets with dimensions of  $\varnothing 25$  mm and length 100 mm were machined

from slabs of Ø348 mm industrial DC cast billet feedstock in the homogenised condition, taking care to avoid sampling too near to the circumference of the billet. For each alloy the same cast number was utilised for all billets as to avoid any variation in the base metal characteristics. The composition of the alloys, determined by means of optical emission spectography is shown in Table 1.

Table 1 composition of alloys (values in weight percentages)

|         | Si   | Fe   | Cu    | Mn    | Mg   | Cr    | Zn    | Ti    |
|---------|------|------|-------|-------|------|-------|-------|-------|
| AA 6060 | 0.46 | 0.22 | 0.003 | 0.028 | 0.51 | 0.003 | 0.016 | 0.010 |
| AA 6082 | 1.08 | 0.19 | 0.019 | 0.490 | 0.69 | 0.100 | 0.014 | 0.017 |

In the trials a flat strip with dimensions 15 x 3 mm was extruded, with an extrusion ratio of 11. A specially designed die was used, as shown in Fig 1, in which a weld seam was formed in the centre of the strip, resulting from a die part containing a single leg perpendicular to the strip orientation fixed in front of the die plate. The dies employed in these experiments featured varying welding chamber depths,  $t$ . Keeping the leg dimensions constant, a deep chamber of  $t = 15$  mm in die B1-15 facilitates a converging metal flow and thus is expected to ease weld-seam formation, while a shallow chamber of  $t = 2$  mm in die B1-2 impedes converging metal flow and hence increases the risk of poorly bonded weld-seams. The flat die B0 produces the same profile geometry; however, as no bridge is incorporated, no weld seam is formed. The properties of the material from this die thus serve as reference values for the samples obtained from other dies.

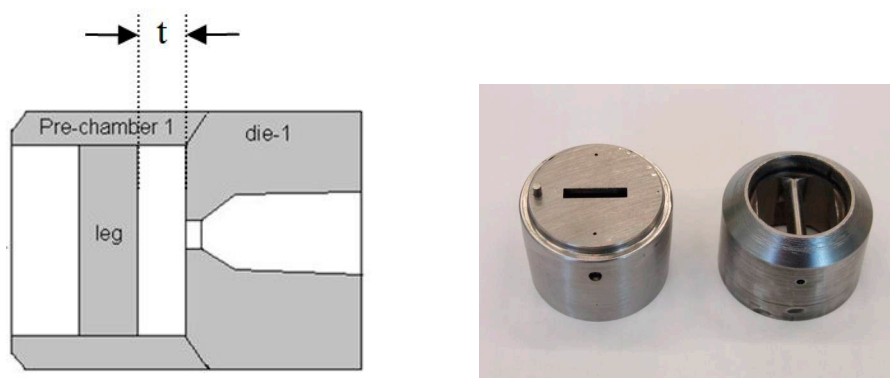


Figure 1 tooling geometry

Tests were performed at pre-set billet temperatures of 450°C and 500°C and a constant ram speed of 1 mm/s. Directly following extrusion, the product was air quenched and subsequently artificially aged to the peak strength (T5) condition. Extrusion was performed in ‘billet-to-billet’ mode, where each consecutive billet was extruded directly onto the previous billet, without removal of any discard. Care was taken in sampling to avoid the incorporation of material originating from the transition area between two billets, containing the transverse welds, by eliminating a liberal portion of the extruded transition length of two consecutive billets.

Mechanical characterisation of the samples was performed by means of transverse tensile tests performed at room temperature and at a fixed crosshead speed. As mentioned previously, the static strength values may not be appropriate for assessment of the bond performance. Therefore the results of the tensile tests were transformed into a modified version of ductility indicator,  $D_v$ , originally developed by Schleich et al. [5], eq. 3. This ductility indicator incorporates the representative features of the tensile curve; that is the uniform strain,  $\epsilon_{gl}$ , the 0.2% proof strain,  $\epsilon_{Rp0.2}$ , the work hardening coefficient  $n$ , the ultimate tensile strength  $R_m$ , the fracture stress  $\sigma_{br}$ , the fracture strain,  $\epsilon_{Br}$ , expressed into a single value when combined with the reduction in the cross-sectional area of the test piece,  $r$ .

$$D_v = \frac{r \cdot \left[ \left( \left[ \ln \frac{[\ln(\varepsilon_{Gl} + 1)]^n}{[\ln(\varepsilon_{Rp0.2} + 1)]^n} \right]^2 + \left[ \ln \frac{\varepsilon_{Gl} + 1}{\varepsilon_{Rp0.2} + 1} \right]^2 \right)^{0.5} + \left( \left[ \ln \left( \frac{R_m}{\sigma_{Bruch}} \right) \right]^2 + \left[ \frac{\ln(\varepsilon_{Br} + 1) - \ln(\varepsilon_{Gl} + 1)}{\ln(\varepsilon_{Gl} + 1)} \right]^2 \right)^{0.25} \right]}{1 + r} \quad (3)$$

Thus Eq. 3 takes into account the work hardening effect and the deformation characteristics of the material prior to the onset of plastic instability (necking), expressed by the first two terms, and the subsequent development of stress and strain following the onset of necking, typified by the following two terms. As the onset of necking is also governed by the stress triaxiality, determined by the geometry of the test piece, the calculated values for  $D_v$  serve as a relative comparison and cannot be compared to results from tests on samples with different geometry.

Cross-sectional samples from the extruded lengths were polished and electrolytically etched for inspection by means of light optical microscopy. The fracture surfaces of the samples were studied by scanning electron microscopy (SEM) in order to relate the morphology of the fracture surface to relevant features of the weld-seams.

## Results and discussion

All extrusions were performed without any irregularities. For both alloys and all die configurations the extrusion trials yielded strips with no obvious extrusion defects such as hot-shortness cracking and die marks and with a bright appearance and good surface finish. The value for the ductility indicator  $D_v$ , calculated from the tensile test data is presented in Fig. 2. The values have been scaled to the maximum value obtained for each alloy.

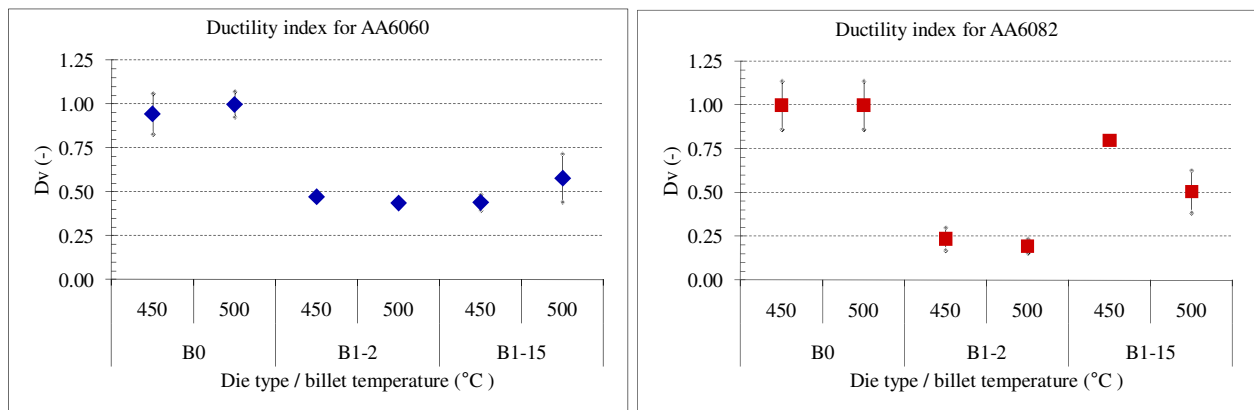


Figure 2 results of the transverse tensile tests, processed into the ductility indicator  $D_v$ ; each data point is an average of at least three individual tests.

For both alloys the highest values for  $D_v$  are obtained for samples from die B0; i.e., the die without a bridge, hence these values are representative for the transverse bulk properties of the extrusions without a weld seam. A decrease is observed in the value for  $D_v$  in all cases where a weld seam is formed in the extrusion. In the case of alloy AA6060,  $D_v$  is reduced to approximately 50% of the value obtained for die B0, with only a slight variation for all cases in which a weld seam is present. In the case of AA6082 the decrease is even more pronounced in the case of die B1-2, where values are reduced by approximately 75%. However, in contrast to alloy AA6060, the ductility index for samples from die B1-15 increases to 75% of the value for  $D_v$  for the non-weld seam samples for extrusions performed at 450°C and to 50% of the reference value obtained for die B0 for extrusions produced with a die temperature of 500°C.

An overview of the cross-sectional microstructures of the extruded sections is shown in Fig. 3. The different response for each alloy to extrusion processing is clearly evident: in the weld seam samples alloy AA6060 exhibits a relatively coarse, recrystallised microstructure, whilst alloy AA6082 retains a heavily deformed, predominantly fibrous microstructure.

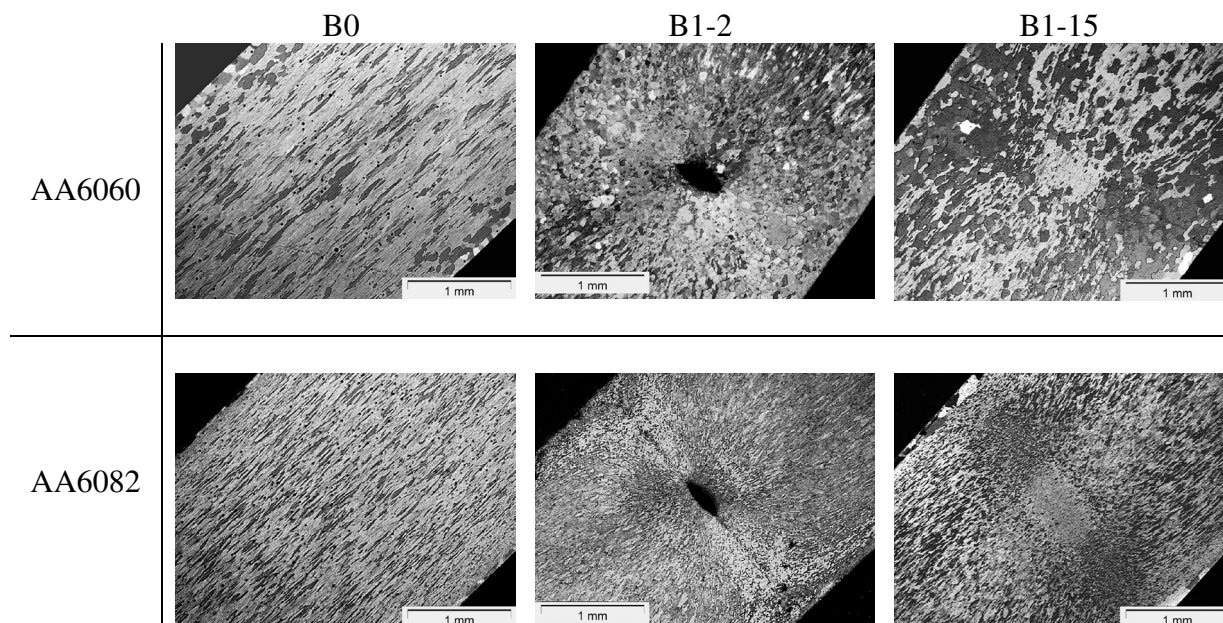


Figure 3 microstructures of extruded samples from the three die geometries and the two alloys

The effect of an obstruction in the die (in his case the bridge to create a weld seam) is readily apparent from the micrographs. Whereas the material extruded through die B0 exhibits a continuous microstructure, a clear delineation of the weld seam can be observed in the microstructure of samples from dies B1-2 and B1-15. Moreover, in the case of die B1-2, a void is present at the mid-centre position of the extrusions. In this die the material flow pattern in the weld chamber is apparently not fully convergent after passing the bridge. Equivalent effects of this flow pattern are also visible in the microstructures from die B1-15. For both alloys the central area of the weld seam has a markedly different structure in comparison with the surrounding area.

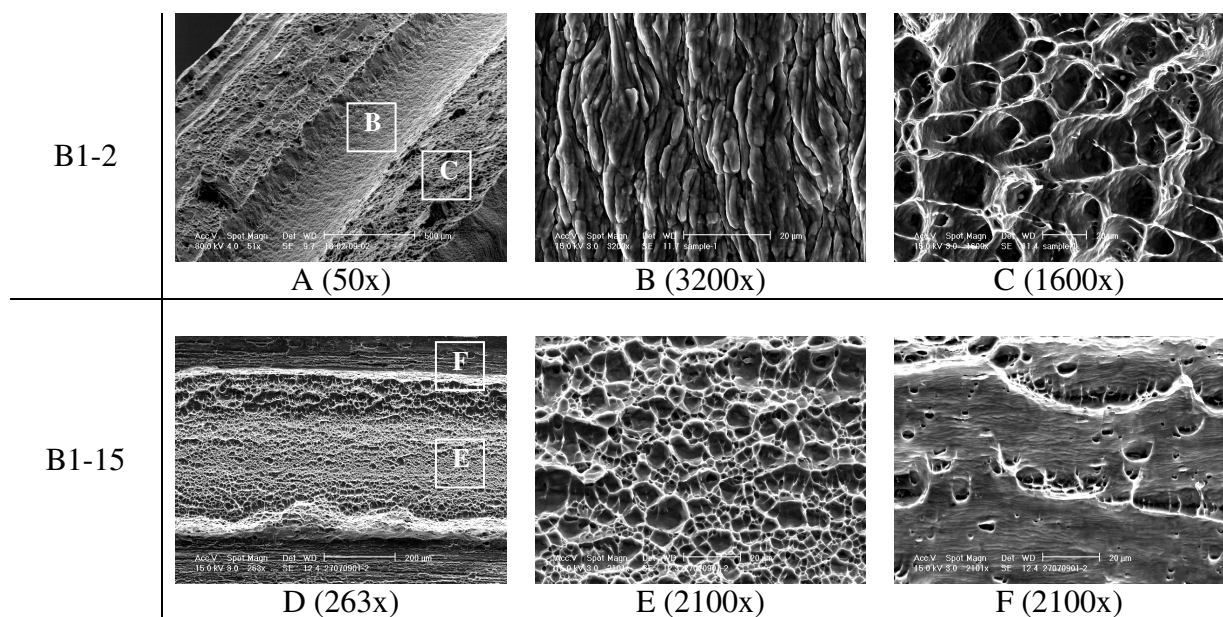


Figure 4 SEM images of fracture surfaces, AA6060; with detailed images of selected locations

Typical images of the fracture surfaces of alloy AA6060 produced with die B1-2 and B1-15 inspected by means of scanning electron microscopy are presented in Fig. 4. The fracture surface of samples from die B1-2 depict a central groove, corresponding with the location of the void, as shown in Fig. 3. The detailed image shown in Fig. 4B confirms the presence of an un-bonded, regular extrusion surface, hence it can be concluded that no contact between the weld planes has occurred in the central area of the extruded strip. Adjacent to this area, as shown in Fig. 4C, a ductile fracture surface is observed. The fracture surface is covered by regularly shaped dimples, of approximately 20  $\mu\text{m}$  in size. The fracture surface of material from die B1-15 also exhibits a central region with a different fracture surface morphology in comparison with the surrounding area. At higher magnification, as shown in Fig. 4E, the central region shows a finely dimpled surface of approximately 5-10  $\mu\text{m}$  in size. The surrounding area, as shown in Fig. 4F, the fracture surface is much smoother, with only some dimples. The morphology of this area suggests a failure process caused by shear deformation after the initial structure has failed due to tensile deformation.

Apart from the non-bonded area in samples from die B1-2, all fracture surfaces show evidence of a ductile fracture process. Evidently, the incompletely bonded surface will impact the value for  $D_v$ , as shown in Fig. 2. In the case of alloy AA6060 the values for  $D_v$  for the material from die B1-15 are on the same level; i.e., the material in the central area does not contribute to the ductility index. Conversely, for alloy AA6082 produced with die B1-15, the values for  $D_v$  improve, especially at the lower billet temperature of 450 °C. Thus in this case, the bond formed in the central area does contribute to the ductility index  $D_v$ . In terms of the weld seam integrity indicator as defined in Eq.1 and Eq.2 it can be stated that  $\alpha I_{ws} \sim 0.50$  for all weld-seams in AA6060 and for the weld-seams from die B1-15 for alloy AA6082,  $\alpha I_{ws} \sim 0.25$  for AA6082, die B1-2 and  $\alpha I_{ws} \sim 0.75$  for AA6082, die B1-15. Obviously,  $I_{ws} < 1$  for die B1-2, as only a partial bond is formed on the weld plane. Further work is aimed at developing  $I_{ws}$  and the damage parameter  $\alpha$ , as to arrive at a quantified prediction of weld seam performance.

## Conclusion

Through an experimental programme the effect of die geometry on the properties of the longitudinal weld-seams has been investigated for alloys AA6060 and AA6082. The application of a ductility index  $D_v$  was shown to be a suitable method to characterize the mechanical performance of the extrusions. The ductility index is obviously negatively influenced in cases where an incomplete weld seam is present due to the formation of a void. Although an improvement in  $D_v$  is observed in some cases where a complete weld seam is formed, other cases still exhibit low values for the ductility index. Therefore it is concluded that detailed insight into the underlying ductile fracture mechanism is required in order to develop a comprehensive predictive weld seam indicator.

## Acknowledgement

This research was partly carried out under the project number MA.08089 in the framework of the Research Programme of the Materials innovation institute M2i.

## References

- 1 R. Akeret, *Journal of the Institute of Metals* 100,(1972) 202-208.
- 2 H. Valberg, T. Loeken, M. Hval, B. Nyhus and C. Thaulow, *International Journal of Materials and Product Technology* 10,(1995) 222-267.
- 3 A. Oosterkamp, L. D. Oosterkamp and A. Nordeide, *Welding Journal*,(2004) 255-261.
- 4 L. Donati and L. Tomesani, *Materials Science Forum* 604-605,(2009) 121-131.
- 5 R. Schleich, T. Keith and M. Liewald, *MP Materials Testing* 50,(2008) 472-476.